Colloid Polym Sci (2005) 284: 26–35
DOI 10.1007/s00396-005-1326-1

ORIGINAL CONTRIBUTION

Raju
Zaheer Khan
Kabir-ud-Din

Kinetics, mechanism and cloud point measurements in the oxidative degradation of non-ionic Triton X-100 surfactant in acidic permanganate solutions

Received: 15 September 2004
Accepted: 15 February 2005
Published online: 13 July 2005

Raju · Z. Khan (✉)
Department of Chemistry,
Jamia Millia Islamia,
New Delhi 110025, India
E-mail: drkhanchem@yahoo.co.in

Kabir-ud-Din
Department of Chemistry,
Aligarh Muslim University,
Aligarh 202002, India

Abstract The polyoxyethylene chain of non-ionic surfactant Triton X-100 [4-(1,1,3,3-tetramethylbutyl) phenyl polyethylene glycol,TX-100] was degraded by permanganate in the presence of $HClO_4$. The oxidative degradation rate and cloud point have been obtained as a function of [surfactant], [permanganate], [$HClO_4$], and temperature. Dependence of the reaction rate on adding inorganic salts ($Na_4P_2O_7$, NaF and $MnCl_2$) was also examined. The oxidation rate increased with increase in [TX-100] and [H^+]. The higher order kinetics with respect to [TX-100] at lower [H^+] shifted to lower order at higher [H^+]. The cloud point of TX-100 (67°C) shifted to lower temperature (23 ± 0.5°C) after oxidative degradation of the polyoxyethylene chain. Evidence of complex formation between TX-100 and MnO_4^- was obtained spectrophotometrically. Presence of the primary alcoholic (–OH) group in the TX-100 skeleton is responsible for the degradation of oxyethylene chain. Both monomeric and aggregated TX-100 molecules are oxidized by permanganate. A catalytic oxidation mechanism is proposed on the basis of the experimental findings.

Keywords Kinetics · Cloud point · Triton X-100 · Permanganate · Oxidation

Introduction

Surfactants are amphipathic molecules having both hydrophobic (water insoluble) and hydrophilic (water soluble) properties. Surfactant properties have attracted growing attention for use in biochemistry, biological and chemical research applications [1]. The chemical stability and the degradability of non-ionic surfactants play an important role in industry [2]. The study of electron transfer processes in organized molecular assemblies (e.g., micelles) has added a new dimension to biochemical research [3–7]. The salient

properties of the surfactants that effect electron transfer reactions are localization and compartmentalization effect, pre-orientational polarity and counter-ion effects and the effect of charged interfaces [8–10]. A number of chemical reactions catalyzed by different types of surfactants have been investigated from the kinetic view point [11–18]. Hidaka et al. reported extensively on the photo-oxidative degradation of surfactants (cationic, anionic and nonionic) catalysed by the TiO_2 semiconductor under either UV irradiation or solar exposure [19, 20].

Considerable kinetic data have accumulated on the oxidative degradation of organic compounds by permanganate ion. However, details of systematic kinetic studies of permanganate oxidation involving micelles (or surfactant monomers) as reductant are not yet well-known. TX-100 (trade name of Union Carbide for [4-(1,1,3,3-tetramethylbutyl) phenyl polyethylene glycol] with average 9.5 moles of oxyethylene and having the lower consolute point (cloud point) at 67°C is easily available and sufficient data exist in literature on the cloud point for a meaningful comparison of the results [21, 22]. In view of our recent results of TX-100 oxidation by Ce(IV) [23], it was thought that it would be of interest to investigate oxidative degradation of the surfactant by another powerful oxidant, viz. acidic permanganate, with a view to having an insight into the mechanism.

We have carried out the present study with the following aims: (1) to determine the effects of different variables on the rates of oxidation of TX-100 (monomer and micelles) by MnO_4^-; (2) to establish formation of colloidal (water soluble) MnO_2 as an intermediate; and (3) to determine the cloud point of TX-100 after degradation. The observed results and the probable explanations are detailed in this paper.

Experimental

Materials

All the reagents used were supplied by Fluka and Merck (India) and were of the commercially available purity. Permanganate solutions were standardized by titration against oxalic acid. The purity of TX-100 was ascertained by the absence of minima in surface tension versus log [TX-100] plots [24]. $HClO_4$ (Thomas Baker, 70% reagent) was used to maintain the $[H^+]$.

Kinetic measurements

Kinetic experiments were carried out at 35°C unless otherwise mentioned. Separately thermostated solution of permanganate and mixture containing TX-100, $HClO_4$ and other reagents (whenever necessary) were mixed. The rate of disappearance of permanganate ion was monitored at 525 nm using cell of path length 1 cm^3. The reactions were usually followed up to the complete disappearance of permanganate color (Fig. 1, inset A). The pseudo-first-order rate constants (k_1 or k_2, s^{-1})–k_1 refers to non-catalytic whereas k_2 refers to autocatalytic reaction pathways) were calculated from the slopes of plots of log (absorbance) versus time. Other details of the kinetic measurements were the same as described elsewhere [16, 25].

Turbidity observations

Visual inspection has been established sufficiently accurately for routine cloud point measurements [26]. Therefore, to observe the appearance of turbidity (cloudiness), different sets of experiments were performed under different conditions. In a typical set, varying amounts of permanganate (up to 66.6×10^{-4} mol dm^{-3}) were mixed with a constant [TX-100] ($=13.3\times10^{-4}$ mol dm^{-3}) and $[H^+]$ ($=0.77$ mol dm^{-3}) at fixed temperature ($=65$°C). Each testing sample was taken in a well-stoppered glass test tube and placed in a thermostated oil bath at the desired temperature. The appearance of clouding was subsequently noted by visual observations. The same procedure was used for different [permanganate], [TX-100] and $[HClO_4]$ at different temperatures ranging from 30°C to 65°C. In addition, the exact cloud point was determined as follows: A sample mixture containing [TX-100] ($=13.3\times10^{-4}$ mol dm^{-3}), $[KMnO_4]$ ($=40.0\times10^{-4}$ mol dm^{-3}), $[H^+]$ ($=0.77$ mol dm^{-3}), for example, was cloudy at 30°C. The system was then allowed to slowly cool and the point of disappearance of clouding was noted.

Results and discussion

Kinetics

Figure 1 shows examples of some of the kinetic curves from which the rate constants for the oxidation were obtained. As the plots of log(absorbance) versus time deviate from linearity, it is clear that the oxidation kinetics proceed in two stages, i.e., initial slow stage followed by a relatively faster step. The time at which the deviation commenced was found to decrease with increase each in $[H^+]$, [TX-100], $[MnO_4^-]$ and temperature. A complete reaction scheme for the oxidation of TX-100 by permanganate is given in Scheme 1.

MnO_4^- + TX-100 ⟶ Intermediate(s) (1)

Intermediate(s) + TX-100 ⟶ Mn(II) + other products (2)

Scheme 1

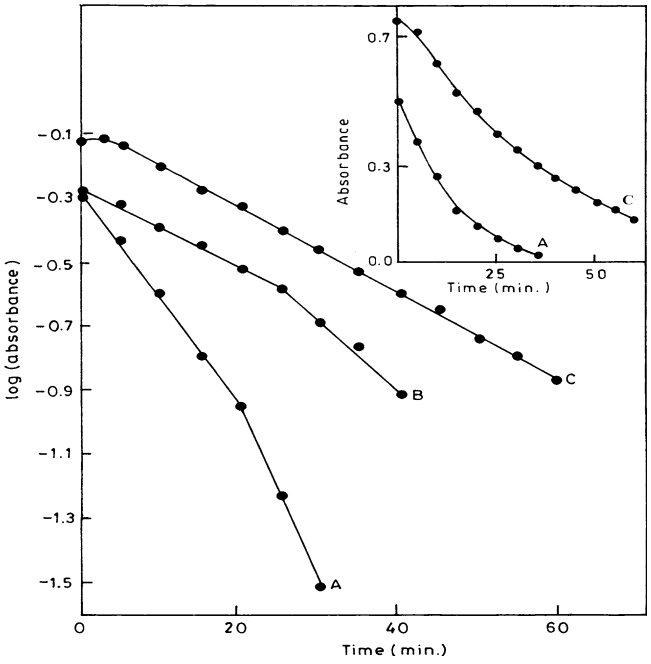

Fig. 1 Plots of log (absorbance) versus time at 525 nm. *Reaction conditions*: $[MnO_4^-] = 2.0\times10^{-4}$ mol dm^{-3}; [TX-100] = 20.0×10^{-4} mol dm^{-3}; $[HClO_4]$ = (A) 6.9, (B) 4.6, (C) 6.9×10^{-2} mol dm^{-3}; $[MnO_2]$ = (A) 0.0, (B) 0.0, (C) 10.0×10^{-5} mol dm^{-3}; temperature = 35°C. *Inset* disappearance of absorbance with time at 525 nm. *Reaction conditions*: same as in Fig 1

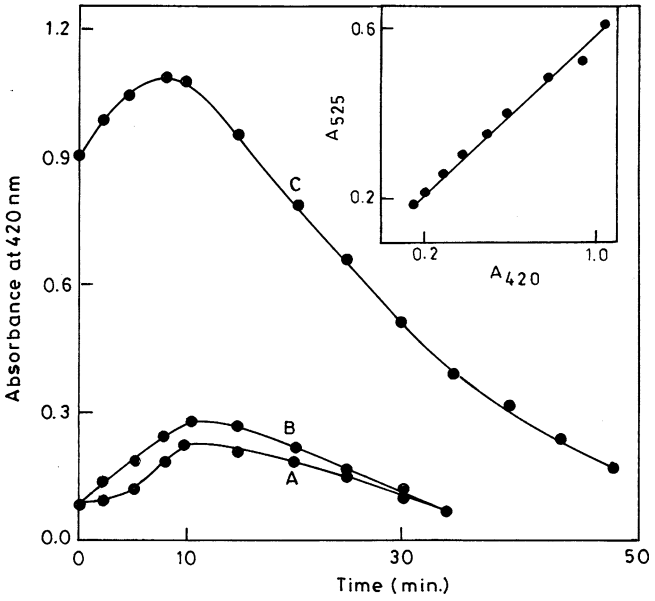

Fig. 2 Plots of absorbance versus time at 420 nm. *Reaction conditions*: $[MnO_4^-] = 2.0\times10^{-4}$ mol dm^{-3}; [TX-100] = 20.0×10^{-4} mol dm^{-3}; $[HClO_4] = 6.9\times10^{-2}$ mol dm^{-3}; [Mn(II)] = (A) 0.0, (C) 0.0, (B) 4.0×10^{-5} mol dm^{-3}; $[MnO_2]$ = (A) 0.0, (B) 0.0, (C) 10.0×10^{-5} mol dm^{-3}. *Inset* absorbance at 525 nm versus absorbance at 420 nm. *Reaction conditions*: [TX-100] = 20.0×10^{-4} mol dm^{-3}; $[MnO_4^-] = 2.0\times10^{-4}$ mol dm^{-3}; $[HClO_4] = 6.9\times10^{-2}$ mol dm^{-3}; temperature = 35°C

It should also be mentioned that ionic strength of the solution could not be maintained constant. In order to avoid complications from precipitation of MnO_2 [27], the reactions were performed in strongly acidic medium. A series of experiments were carried out under different experimental conditions (Figs. 1, 2, 3 and Tables 1, 2). The linearity of both the stages (noncatalytic (k_1) and autocatalytic (k_2)) in the plots of log(absorbance) versus time indicates unit order with respect to $[MnO_4^-]$ in both the stages. On the other hand, it was also observed that rate constants k_1 and k_2 decreased as the initial concentration of MnO_4^- increased (Table 1). The basic trend in chemical kinetics is that the pseudo-first-order rate constants are independent of the initial concentration of the reactant. The same type of defect has been obtained in many permanganate reactions and especially in those having an autocatalytic character [27]. The k_1 and k_2 increased considerably with increasing $[HClO_4]$ (Table 1) and the plots of log (rate constant) versus log $[HClO_4]$ were linear with slopes 1.5 and 1.0 for noncatalytic and autocatalytic steps, respectively. Pseudo-first-order rate constants were found to increase with increasing [TX-100]. The effect of variation of [TX-100] indicates that order with respect to [TX-100] decreases with increasing $[H^+]$ (1.5, 1.3, 1.0 (k_1) and 2.6, 2.0, 1.3 (k_2) with $[H^+] = 2.3$, 4.6, and 6.9×10^{-2} mol dm^{-3} for the noncatalytic and autocatalytic reaction pathways), suggesting involvement of H^+ prior to the electron-transfer step (the rate determining step) for both the stages. In order to confirm the oxidation of TX-100 monomer, some experiments were also performed at [TX-100] < cmc. Interestingly, the autocatalytic part (k_2) is not observed at lower [TX-100]. The values of k_{obs} ($\times10^{-4}$) at 35°C were 0.76, 1.5, 2.3, 3.0 and 3.8 s^{-1} at [TX-100] ($\times10^{-4}$) = 2, 4, 6, 8 and 10 mol dm^{-3}. Thus, permanganate may oxidize both the monomeric TX-100 as well as aggregated units. The rate constants were obtained at 35, 45 and 55°C and, from the plots of log k_1 and k_2 against $1/T$ the values of activation energies (E_a) and other parameters for both the stages were evaluated (Table 1).

Stoichiometry

The reaction stoichiometry was determined using spectrophotometric titrations. Several reaction mixtures with

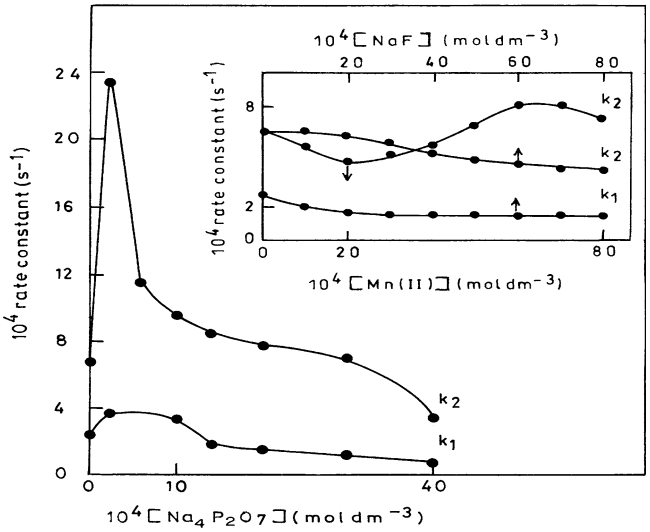

Fig. 3 Plots of rate constants versus [$Na_4P_2O_7$]. *Inset* rate constants (k_1 and k_2) versus [NaF] and rate constant (k_2) versus [Mn(II)]. *Reaction conditions*: $[MnO_4^-] = 2.0\times10^{-4}$ mol dm^{-3}; [TX-100] $= 30.0\times10^{-4}$ mol dm^{-3}; $[HClO_4] = 2.3\times10^{-2}$ mol dm^{-3}; temperature = 35°C

$[MnO_4^-] > [\text{TX-100}]$ (6.0×10^{-4}– 66.6×10^{-4} mol dm^{-3} oxidant: 6.0×10^{-4} mol dm^{-3} reductant) at constant $[H^+]$ ($= 0.77$ mol dm^{-3}) were prepared and kept for 30 min at 60°C. The residual absorbance of MnO_4^- was monitored at 525 nm where there was no absorbance from the Mn(II) species. The stoichiometry for the oxidative degradation of TX-100 by MnO_4^- is 1:3 (TX-100:MnO_4^-).

Spectroscopic evidence for complex formation between MnO_4^- and TX-100

Under the experimental kinetic conditions of $[H^+] = 2.3\times10^{-2}$– 6.9×10^{-2} mol dm^{-3}, there was no spectroscopic and kinetic evidence (strict first-order dependence on [TX-100] and $[H^+]$) in favor of intermediate complex formation between the reactants. However, at lower $[H^+]$ ($= 1.2\times10^{-2}$ mol dm^{-3}), a complex formation was confirmed from initial absorbance increase at 525 nm. Preliminary observations indicate that the absorbance of permanganate ($= 2.0\times10^{-4}$ mol dm^{-3}) changes with [TX-100] ($\geq 2.0\times10^{-3}$ mol dm^{-3}). The initial rapid reaction may be represented as

$$MnO_4^- + \text{TX-100} \overset{K_c}{\rightleftharpoons} \text{complex} + H_2O \qquad (3)$$

At constant $[H^+]$, the value of complex formation constant (K_c) was determined by using the relation [28]

$$\frac{[MnO_4^-]_T[\text{TX-100}]}{\Delta A} = \frac{[\text{TX-100}]}{\Delta\varepsilon l} + \frac{1}{K_c\Delta\varepsilon l} \qquad (4)$$

where, ΔA = the difference in absorbance between the complex and Mn(VII) species at the wavelength ($\lambda_{max} = 525$ nm) when both the uncomplexed and complexed forms of Mn(VII) absorb, $\Delta\epsilon$ = the difference in absorption coefficients, and l = the path length. To test the validity of Eq. 4, the left-hand-side term was plotted against [TX-100], which was found to be fairly linear. From the slope and intercept, the values of K_c and $\Delta\epsilon$ were calculated and found to be 14.8×10^3 mol^{-1} dm^3 and 800 mol $^{-1}$dm^3 cm^{-1}, respectively.

Table 1 Values of the pseudo-first-order rate constants (k_1 and k_2) and activation parameters (E_a, $\Delta H^{\#}$, $\Delta S^{\#}$) for the oxidation of TX-100 ($= 30.0\times10^{-4}$ mol dm^{-3}) by permanganate

10^4 [MnO_4^-] (mol dm^{-3})	10^2 [$HClO_4$] (mol dm^{-3})	Temp (°C)	10^4 k_1 (s^{-1})	10^4 k_2 (s^{-1})
1.0	2.3	35	3.2	7.0
1.5	2.3	35	3.8	6.8
2.0	2.3	35	2.4	6.5
2.5	2.3	35	2.3	6.3
3.0	2.3	35	1.9	6.0
2.0	2.3	35	2.4	6.5
2.0	3.0	35	3.2	8.0
2.0	4.6	35	6.1	10.7
2.0	6.0	35	9.6	15.9
2.0	6.9	35	12.2	19.1
2.0	2.3	35	2.4	6.5
2.0	2.3	45	3.8	9.5
2.0	2.3	55	7.6	13.0
Activation parameters			Noncatalytic	Autocatalytic
E_a (kJ mol^{-1})			49	28
$\Delta H^{\#}$ (kJ mol^{-1})			46	25
$-\Delta S^{\#}$ (J K^{-1} mol^{-1})			300	298

Table 2 Values of the pseudo-first-order rate constants ($k_1$and k_2) at different [TX-100] at three different [$HClO_4$] for the oxidation of TX-100 by permanganate ($=2.0\times10^{-4}$ mol dm^{-3}) at 35°C

10^4 [TX-100] (mol dm^{-3})	10^2 [$HClO_4$] (mol dm^{-3})					
	2.3		4.6		6.9	
	10^4 k_1 (s^{-1})	10^4 k_2 (s^{-1})	10^4 k_1 (s^{-1})	10^4 k_2 (s^{-1})	10^4 k_1 (s^{-1})	10^4 k_2 (s^{-1})
14	0.0	0.0	2.2	3.6	5.3	11.5
20	0.9	2.5	3.0	6.5	9.2	14.5
26	1.8	4.8	5.0	8.8	10.2	16.4
30	2.3	6.5	6.1	10.7	12.2	19.1
40	3.8	13.8	9.2	19.9	16.1	28.4
44	4.2	17.2	10.2	24.5	18.2	32.4
50	5.0	24.2	12.2	29.9	20.1	37.4

Identification of the autocatalysis and formation of manganese(IV)

Additional experiments are needed to determine the true nature of the inflection in the plot of log(absorbance) versus time (Fig. 1a, b), which may arise due to involvement of intermediate(s). These intermediate(s) can lead to cyclic reactions that may result in autocatalysis. In order to identify the intermediate(s), the absorbance of the solutions were monitored at two wavelengths (420 and 525 nm) as a function of time in the absence and presence of the water soluble form of colloidal MnO_2, which was prepared as detailed by Perez-Benito et al. [29]. The observed results are graphically represented in Fig. 2 as absorbance–time profiles. The plots show gradual increase of absorbance with the increase in time up to ca. 10 min at 35°C in the absence(Fig. 2a, b) and presence of colloidal MnO_2 in the reaction mixture (Fig. 2c) at the beginning of the experiments. However, after this optimum time, the absorbances decrease with time. This behavior may be the indication of the formation of Mn(IV) as an intermediate. Permanganate ion is almost transparent to radiation at 420 nm. It can be seen that if MnO_2 is present at the beginning of the reaction (Fig. 2c), the absorbance at 420 nm is higher (Fig. 2a). On the other hand, the plot of log (absorbance) versus time is a straight line (Fig. 1c, instead of the deviation, Fig. 1a, b). On the basis of these observations, we may thus conclude that the intermediate from the reduction of MnO_4^- by TX−100 is Mn(IV) species. The linear relationship between absorbances at 420 and 525 nm (Fig. 2, inset) also indicates that MnO_4^- is converted to highly unstable Mn(V), which goes very rapidly to MnO_2 and that the species which absorbs light at 420 and 525 nm is soluble (colloidal) MnO_2. Formation of Mn(VI) and Mn(V) are ruled out because these species are highly unstable in acidic medium [30].

In order to further confirm/gain insight into the autocatalytic pathway, the effect of initially added Mn(II) (reduction product of MnO_4^-) was also studied. The results, shown in Fig. 3 as rate constant—[Mn(II)] profile, indicate sigmoid dependence of k_2 on [Mn(II)]. It was also noticed that the extent of the noncatalytic reaction pathway disappeared completely. Our results seem to indicate that Mn(II) is a true active autocatalyst (the Mn(II) formed as reaction product contributes to accelerate the oxidation of TX-100 by MnO_4^-).

It is well-known that Mn(III) species is reasonably stable only in acidic solution (pH < 3.0) and disproportionate in solutions of higher pH [31]. Therefore, to substantiate the formation of Mn(III) as an intermediate during the present reaction, the effects of adding [$P_2O_7^{4-}$] and [F^-] were investigated. It is seen that rate constants decrease with increase in [$P_2O_7^{4-}$] and [F^-] (Fig. 3). The observed inhibitory effects suggest the possibility of formation of Mn(III) (although our attempts failed to observe appearance of this ion at 470 nm—the λ_{max} for aqua manganese(III). This indicates that Mn(III) may also be the reactive species in the autocatalytic path. Therefore, it can be concluded that the oxidation of TX-100 by MnO_4^- is autocatalysed by soluble colloidal MnO_2 and Mn(III) (formed as the reaction intermediates) and Mn(II) (formed as reaction product).

During the oxidation of TX-100 it was noticed that the order with respect to TX-100 decreases with increasing [H^+], which shows that the involvement of H^+ must be considered before the rate-determining step. In a strong or moderate acid medium, MnO_4^- ion is protonated in accordance with the equilibrium $MnO_4^- + H^+ \rightleftharpoons HMnO_4$ to afford $HMnO_4$ (which is a powerful oxidant).

On the basis of experimental results the following two mechanisms can be proposed:

1. Noncatalytic reaction pathway

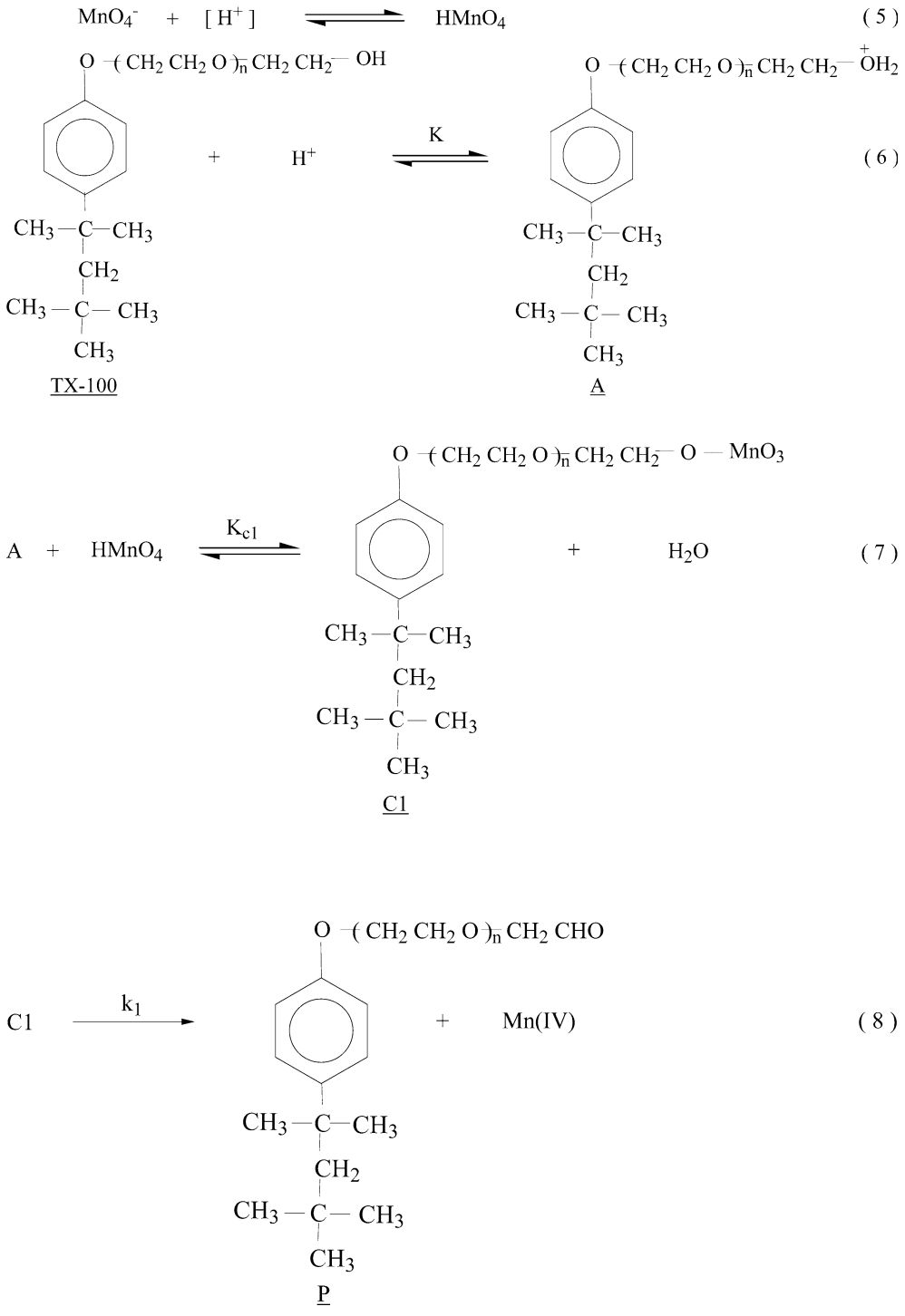

Scheme 2

2. Autocatalytic reaction pathway

$$MnO_2 + \text{TX-100} \underset{}{\overset{K_{c2}}{\rightleftharpoons}} MnO_2\text{-TX-100} \quad (9)$$

C2

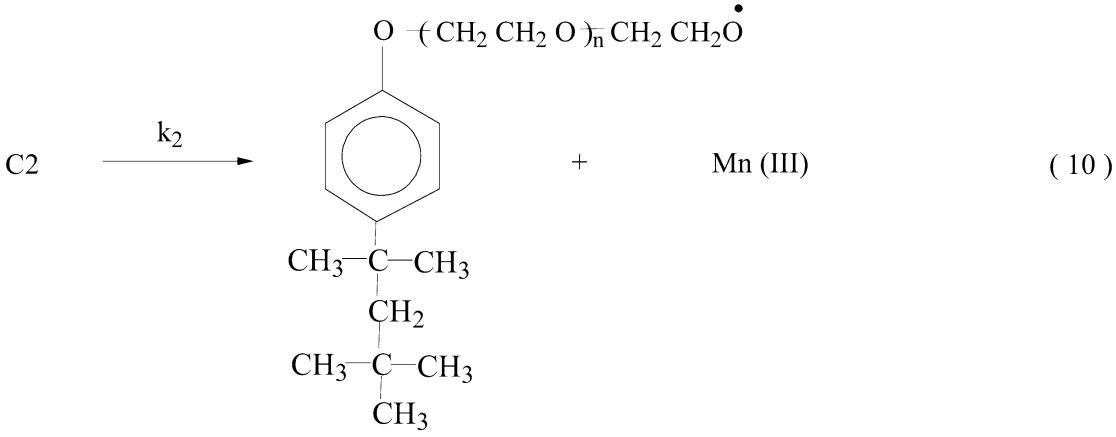

$$\text{Mn (III)} + \text{TX-100} \xrightarrow{\text{fast}} \text{Mn(II)} + \text{P} \quad (11)$$

$$\text{Mn (III)} + \text{Radical} \xrightarrow{\text{fast}} \text{Mn(II)} + \text{P} \quad (12)$$

$$\text{Mn (IV)} + \text{Mn (II)} \longrightarrow 2\ \text{Mn (III)} \quad [\text{ref. 32}] \quad (13)$$

$$MnO_4^- + 4\ \text{Mn(II)} + 8\ H^+ \longrightarrow 5\ \text{Mn (III)} + 4\ H_2O \quad [\text{refs.33,34}] \quad (14)$$

$$2\ MnO_4^- + 3\ \text{Mn(II)} + 2\ H_2O \longrightarrow 5\ MnO_2 + 4\ H^+ \quad [\text{ref.35}] \quad (15)$$

Scheme 3

In Scheme 2, Eqs. 5 and 6 represent, respectively, protonations of MnO_4^- and TX-100. The next reaction shows formation of a 1: 1 TX-100-Mn(VII) complex (C1). In analogy with previous studies [32], we assume that it decomposes to Mn(IV) and product (P) (other oxidation states of Mn are obviously involved in the reaction; they are extremely reactive and unstable in acidic solutions). It is worth mentioning that Scheme 2 mechanism is valid only for higher $[H^+]$ (first-order with respect to [TX-100]).

From the Scheme 2 mechanism the following rate-law is derived:

$$k_{obs1} = \frac{k_1 K_{c1} K[H^+][\text{TX-100}]_T}{(1 + K[H^+])} \quad (16)$$

Under the experimental conditions of $[H^+] = 2.3\times10^{-2}$ mol dm^{-3}, $1 > K\ [H^+]$, and Eq. 16 reduces to

$$k_{obs1} = k_1 K_{c1} K[H^+][\text{TX-100}]_T \quad (17)$$

Equation 17 clearly explains the first-order dependence of the reaction each on $[H^+]$ and $[\text{TX-100}]_T$. At constant $[H^+]$ ($=2.3\times10^{-2}$ mol dm^{-3}), the value of k_1K, obtained from the slope ($=0.38$) of the plot of rate constant (k_{obs1}) versus [TX-100], was found to be 1.11×10^{-3} mol^{-1} dm^3 s^{-1} .

In Scheme 3, reaction (9) represents formation of another complex (C2) with the colloidal MnO_2 and TX-100. Equation 10 is the rate determining step of autocatalytic pathway to yield Mn(III) as an intermediate. Therefore, Mn(III) would also participate in the reaction as an autocatalyst. In the presence of large amount of TX-100, the intermediate (Mn(III)) immediately gets converted into stable products (Eq. 11). The reduction of colloidal MnO_2 to Mn(III) by Mn(II) has also been reported by Perez-Benito [32]. Our results seem to suggest that there is a competition between Mn(II) and TX-100 to react with MnO_4^- (reactant) and colloidal MnO_2 (intermediate). Interestingly, Scheme 3 clearly indicates that the autocatalytic is not a true path of the MnO_4^-—TX-100 reaction. It may be a mixture of a series of cyclic reactions (Eqs. 9, 10, 11, 12, 13, 14, 15). Therefore, the exact dependence of k_2 on [TX-100] and $[H^+]$ cannot be estimated. Thus, we conclude that if externally added Mn(II) is present in the reaction mixture at the beginning of the experiments, the path of permanganate reactions may become more complicated. However, from Scheme 3 mechanism the following rate equation is derived:

$$k_{obs2} = \frac{k_2 K_{c2} K[H^+][\text{TX-100}]_T}{(1 + K[H^+])} \quad (18)$$

At constant $[H^+]$, the rate law, Eq. 18, is thus reduced to Eq. 19.

$$k_{obs2} = k_2 K_{c2} K[H^+][\text{TX-100}]_T \quad (19)$$

This clearly explains the first-order dependence of reaction each on $[H^+]$ and [TX-100] in the autocatalytic reaction pathway.

The value of $\Delta S^{\#}$ for both steps (noncatalytic and autocatalytic) are the same (Table 1) whereas the noncatalytic step is associated with a higher $\Delta H^{\#}$ than the autocatalytic. Thus, the oxidation is enthalpy-controlled rather than an entropy- controlled one. On the other hand, large negative value of $\Delta S^{\#}$ suggests a bimolecular reaction in the rate-determining step in the presence of water as solvent and the involvement of proton transfer during the rate-determining step for the acid-catalyzed reactions.

Oxidative degradation of polyoxyethylene chain of TX-100

The main body of the TX-100 surfactant is composed of saturated alkyl $\{(CH_3)_3C\text{-}CH_2C(CH_3)_2\text{–}\}$ and polyoxyethylene $\{(OCH_2CH_2)_n\}$ chains. The saturated alkyl chain has been considered to be relatively stable under normal conditions. However, it should be added that the alkyl chain of nonionic surfactants is not necessarily immune to degradation. The activating substituents (unsaturation and aromaticity) can increase their reactivity under sufficiently vigorous conditions [36]. In general, the rapidity of the reaction in the ether chains permits the alkyl chain reaction to be neglected. In fact, the polyether chains show behavior similar to that of simple ethers, undergoing auto-oxidation very readily. It has been established that the cloud points of nonionic surfactants may decrease and increase after the shortening of polyoxyethylene- and saturated alkyl chains [2]. In order to confirm these facts, a series of experiments were performed to determine the cloud point under various experimental conditions. These results are given in Fig. 4 and Table 3. It was observed that at specific concentrations of TX-100, $HClO_4$ and $KMnO_4$, the reaction mixture became cloudy. The time of the appearance of turbidity decreased with increasing temperature (Fig. 4). It was also noticed that turbidity did not appear at all at 20°C even after prolonged incubation at this temperature. Under our experimental conditions, however, the cloud point of TX-100 ($=13.3\times10^{-4}$ mol dm^{-3}) is 23°C in presence of MnO_4^- ($=40.0\times10^{-4}$ mol dm^{-3}) and $[H^+]$ ($=0.77$ mol dm^{-3}). Therefore, it was safe to assume that there was no pure TX-100 surfactant (cloud point = 67°C). From Fig. 4, it

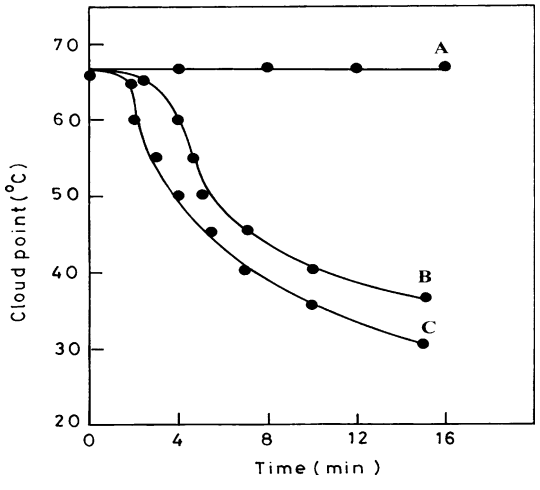

Fig. 4 Plots of temperature of turbidity appearance versus time. *Reaction conditions*: $[\text{TX-100}] = 13.3\times10^{-4}$ mol dm^{-3}; $[HClO_4] = 0.77$ mol dm^{-3}; $[MnO_4^-]$ = (A) 0.0, (B) 33.3, (C) 40.0×10^{-4} mol dm^{-3}

Table 3 Effects of $[MnO_4^-]$, [TX-100] and $[H^+]$ on the appearance of turbidity for the oxidative degradation of TX-100 by permanganate in the presence of $HClO_4$ at different temperatures

10^4 $[MnO_4^-]$ (mol dm^{-3})	10^4 [TX-100] (mol dm^{-3})	$[HClO_4]$ (mol dm^{-3})	Appearance of turbidity[a]			
			Temperature (°C)			
			30	40	50	60
0.0	13.3	0.0	N	N	N	N
0.0	13.3	0.77	N	N	N	N
6.0	13.3	0.77	N	N	N	O
11.6	13.3	0.77	N	N	N	O
13.3	13.3	0.77	N	N	N	O
20.0	13.3	0.77	O	O	O	O
26.6	13.3	0.77	O	O	O	O
32.2	13.3	0.77	O	O	O	O
40.0	13.3	0.77	O	O	O	O
53.3	13.3	0.77	D	D	D	D
66.6	13.3	0.77	D	D	D	D
40.0	13.3	0.15	N	N	N	N
40.0	13.3	0.38	O	O	O	O
40.0	13.3	0.62	O	O	O	O
40.0	13.3	0.77	O	O	O	O
40.0	13.3	1.16	O	O	O	O
40.0	13.3	1.15	N	N	N	N
40.0	13.3	1.93	N	N	N	N
40.0	6.6	0.77	D	D	D	D
40.0	13.3	0.77	O	O	O	O
40.0	20.0	0.77	O	O	O	O
40.0	26.6	0.77	N	N	N	N
40.0	33.3	0.77	N	N	N	N
40.0	40.0	0.77	N	N	N	N
40.0	46.6	0.77	N	N	N	N
40.0	53.3	0.77	N	N	N	N
40.0	60.0	0.77	N	N	N	N

[a]Turbidity test: *N* no turbidity, *O* turbidity observed, *D* MnO_2 deposition

is seen that $HClO_4$ has no effect on the cloud point, while addition of permanganate in the same solutions has a drastic effect on the cloud point. This is a clear indication that decrease in the cloud point is due to the degradation of polyoxyethylene chain of TX-100 which, in turn, changes the nature of the micelles. Reaction mixtures become turbid at 30°C as scission reduces the HLB below critical value. Thus, it is safe to conclude that the free radical generated in the oxidation of TX-100 by permanganate, undergoes cleavage [2] at C–O bond of polyoxyethylene chain of TX-100, which, in turn, decreases the cloud point of this surfactant. On the basis of decrease in cloudpoint and previous hypothesis [2], the following additional step (kinetically indistinguishable) cannot be ruled out, especially in the presence of a strong oxidizing agent, such as permanganate. Mixing of TX-100 and MnO_4^- produces a complex series of reactions. The ether groups of polyoxyethylene of TX-100, which are prone to form peroxides, are the sites of initial attack of MnO_4^-. Aldehyde group can form from the scission of the polyoxyethylene chain as well as from oxidation of the primary hydroxyl group. In the

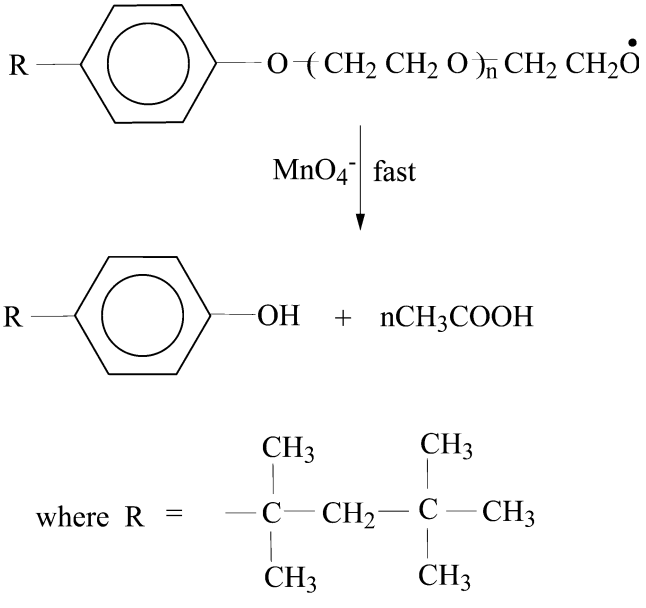

Scheme 4

presence of permanganate, the oxidation of –CHO group would continue to produce the carboxylic acid.

Cleavage of the C–O bond of oxyethylene chain of the nonionic surfactant should undoubtedly disturb hydrophilic–lipophilic balance, the cmc and the cloud point but the change may not necessarily occur smoothly (Table 3). Primary alkoxy radical is stable enough at ambient temperature to form the alcohol by H-abstraction from the other molecule of TX-100. Presence of carboxylic group (–COOH) in the degraded solution was detected by spot test. In our attempt to confirm the aldehyde, Nash's procedure [37] was also used: the reaction mixture was treated with acetylacetone, acetic acid and ammonium acetate following which the absorbance of the resulting diacetyl dihydrolutidine was monitored at 415 nm.

In order to confirm the oxidative degradation of ether linkage in TX-100, some additional experiments were also carried out in presence of diethyl ether. In a typical experiment, [MnO_4^-] (2.0×10^{-4} mol dm^{-3}) was mixed with diethyl ether (20% v/v) at room temperature (28°C). It was found that the permanganate color disappeared completely, which indicated the instability of the polyoxyethylene chain of TX-100 (vide supra, Scheme 4).

Conclusion

The most interesting feature of this study is the oxidation of TX-100 by MnO_4^-. We are unaware of precedence in the redox chemistry of TX-100. The linearity in the plot of log(absorbance) versus time at 525 nm in the presence of colloidal MnO_2 in solution at the beginning of the experiments is unique in the sense that reaction has no induction period. The presence of –OH group in the polyoxyethylene chain of TX-100 is responsible for the oxidative degradation. The degradation in the polyoxyethylene chain is best understood by an examination of cloud point of the non ionic surfactant. Cloud point of TX-100 decreases sharply in the presence of MnO_4^- with time. This study opens up a new area of surfactant science in which surfactants can be used as a reactant. Similar detailed studies may contribute towards biodegradability of such molecules.

References

1. Attwood D, Florence AT (1983) Surfactant systems their chemistry, pharmacy and biological properties. Chapman and Hall, NY
2. Donbrow M (1987) In: Schick MJ (ed) Nonionic surfactants: physical chemistry, surfactant science series, vol 23, Chapter18. Marcel Dekker, NY
3. Piszkiewicz D (1977) J Am Chem Soc 99:7695
4. Richmond W, Tondre C, Krzyzanowska E, Szymanowski J (1995) J Chem Soc Faraday Trans 91:657
5. Vinokurov IA, Kankare J (2002) Langmuir 18:6789
6. Shukla RS, Pant RP (2003) J Colloid Interf Sci 268:168
7. Herszage J, Afonso MD (2003) Langmuir 19:9684
8. Fendler JH (1982) Membrane mimetic chemistry, characterization and applications of micelles, microemulsions, monolayers, bilayers, vescicles, host-guest systems and polyions. Wiley, NY
9. Rodriguez A, Moya ML (1996) Langmuir 12:4090
10. Kabir-ud-Din, Hartani K, Khan Z (2001) Colloids Surf A Physicochem Eng Aspects 193:1
11. Menger FM, Portnoy CE (1967) J Am Chem Soc 89:4098
12. Bunton CA, Minch M, Sepulveda L (1971) J Phys Chem 75:2707
13. Perez-Benito E, Rodenas E (1991) Langmuir 7:232
14. Bunton CA (1997) J Mol Liq 72:231
15. Khan MN, Arifin Z, Lasidek MN, Hanifiah MAM, Alex G (1997) Langmuir 13:3959
16. Kabir-ud-Din, Salem JKJ, Kumar S, Rafiquee MZA, Khan Z (1999) J Colloid Interf Sci 213:20
17. Dubey DK, Gupta AK, Sharma M, Prabha S, Vaidyanathaswamy R (2002) Langmuir 18:10489
18. Bunton CA, Gillitt ND (2002) J Phys Org Chem 15:29
19. Hidaka H, Zhao (1992) J Colloids Surf A Physicochem Eng Aspects 67:165
20. Zhao Z, Hidaka H, Takamura A, Pelizzeti E, Serpone N (1993) Langmuir 9:1646
21. Schott H (1998) J Colloid Interf Sci 205:496
22. Goel SK (1999) J Colloid Interf Sci 212:406
23. Khan Z, Raju, Kabir-ud-Din (2003) Colloids Surf A Physicochem Eng. Aspects 225:75
24. Harrold SP (1960) J Colloid Sci 15:280
25. Kabir-ud-Din, Salem JKJ, Kumar S, Rafiquee MZA, Khan Z (1999) J Colloid Interf Sci 215:9
26. Schott H (1997) J Colloid Interf Sci 189:117
27. Perez-Benito JF, Arias C, Amat E (1996) J Colloid Interf Sci 177:288
28. Lin CT, Beattie JK (1972) J Am Chem Soc 94:3011
29. Perez-Benito JF, Arias C (1992) J Colloid Interf Sci 149:92
30. Simandi LI, Jaky M (1976) J Am Chem Soc 98:1995
31. Lune-Pereira C, Baral S, Hengylein A, Janata E (1985) J Phys Chem 89:5772
32. Perez-Benito JF (2002) J Colloid Interf Sci 248:130
33. Powell RT, Oskin T, Ganapathisubramanian N (1989) J Phys Chem 93:2718
34. Rosseinsky DR, Nicol MJ (1965) Trans Faraday Soc 61:2718
35. Perez-Benito JF, Arias C, Brillas E (1990) Int J Chem Kinet 22:261
36. Scott G (1965) Atmospheric oxidation and antioxidants Elsevier, Amsterdam
37. Hidaka H, Zhao J, Pelizzetti E, Serpone N (1992) J Phys Chem 96:2226